informa
healthcare

Reduced chromosome aberration complexity in normal human bronchial epithelial cells exposed to low-LET γ-rays and high-LET α-particles

Matthew Themis[1,2], Elisa Garimberti[1], Mark A. Hill[3] & Rhona M. Anderson[1,2]

[1]*Centre for Cell Chromosome Biology,* [2]*Centre for Infection, Immunity and Disease Mechanisms, Division of Biosciences, Brunel University, West London, and* [3]*CRUK/MRC Gray Institute for Radiation Oncology & Biology, Department of Oncology, University of Oxford, Oxford, UK*

Abstract

Purpose: **Cells of the lung are at risk from exposure to low and moderate doses of ionizing radiation from a range of environmental and medical sources. To help assess human health risks from such exposures, a better understanding of the frequency and types of chromosome aberration initially-induced in human lung cell types is required to link initial DNA damage and rearrangements with transmission potential and, to assess how this varies with radiation quality.**

Materials and methods: **We exposed normal human bronchial lung epithelial (NHBE) cells *in vitro* to 0.5 and 1 Gy low-linear energy transfer (LET) γ-rays and a low fluence of high-LET α-particles and assayed for chromosome aberrations in premature chromosome condensation (PCC) spreads by 24-color multiplex-fluorescence *in situ* hybridization (M-FISH).**

Results: **Both simple and complex aberrations were induced in a LET and dose-dependent manner; however, the frequency and complexity observed were reduced in comparison to that previously reported in spherical cell types after exposure to comparable doses or fluence of radiation. Approximately 1–2% of all exposed cells were categorized as being capable of transmitting radiation-induced chromosomal damage to future NHBE cell generations, irrespective of dose.**

Conclusion: **One possible mechanistic explanation for this reduced complexity is the differing geometric organization of chromosome territories within ellipsoid nuclei compared to spherical nuclei. This study highlights the need to better understand the role of nuclear organization in the formation of exchange aberrations and, the influence three-dimensional (3D) tissue architecture may have on this *in vivo*.**

Keywords: M-FISH, geometry of cell nucleus, radiation exposure, human lung

Introduction

Lung cancer is the most common cause of cancer mortality in males and the second most common cause in women principally due to the lack of early diagnosis (Travis et al. 1995). The highest risk factor for lung cancer is cigarette smoking, but with increasing public awareness individuals smoking habits are changing (Peto et al. 2000) and it is suggested that worldwide 25% of lung cancers cannot be attributed to tobacco use (Sun et al. 2007). A known non-smoking risk factor for lung carcinogenesis is exposure to radon gas and its daughters. Indeed uranium miner data, where workers have been exposed to relatively high doses of high-linear energy transfer (LET) radiation, has established a causal relationship between radon exposure and lung cancer (National Research Council [NRC] 1998, Tomasek and Placek 1999) while studies carried out by Darby et al. observed a causal relationship between radon exposure in the home and the occurrence of lung cancer, estimating radon to account for 9% of all lung cancer deaths in Europe (Darby et al. 2005, 2006). A further study carried out in the USA similarly demonstrates a causal association between domestic radon exposure and lung cancer (Krewski et al. 2006).

The lung is also a potential target for radiation exposure during medical examination, e.g., chest X-rays (0.01–0.15 mGy), computerized tomography (CT) scans (40–100 mGy) (Hall and Brenner 2008) and fluoroscopic interventional procedures (0.5–6 mSv) (Beels et al. 2009, Steinfort et al. 2010). Additionally, the lung may be irradiated as part of external beam radiotherapy with the dose to the lung varying significantly depending on whether the lung is in or out of the treatment field (Taylor and Kron 2011). The quantitative relationship between such exposure and the occurrence of secondary

treatment-related cancers is not known. However there is evidence of an excess of lung cancers in long-term survivors with primary breast cancer or Hodgkins disease after treatment with ionizing radiation (NRC 2006, Xu et al. 2008).

Accordingly, understanding the biology of radiation-induced lung cancer is becoming ever more important. Structural chromosome aberrations are known to be very effectively induced after exposure to ionizing radiation whereby the frequency and type induced and subsequently transmitted, varies depending on radiation dose, radiation quality, cell type and cell cycle stage of at time of irradiation (Griffin et al. 1995, Anderson et al. 2000, 2003, Boei et al. 2001, Loucas and Cornforth 2001, Ritter et al. 2002a, Wu et al. 2003a, Duran et al. 2009, George et al. 2010, Loucas et al. 2013, and references therein). Similarly, the relationship between chromosome aberrations with the aetiology and progression of many cancers, and in estimating cancer risks, is well established (International Commission on Radiological Protection [ICRP] 2005, Mitelman 2005, Bonassi et al. 2008). The majority of human cancers are epithelial in origin therefore we elected to expose normal human bronchial lung epithelial (NHBE) cells *in vitro* to low-LET γ-rays and a low fluence of high-LET α-particles and assay to determine the frequency and type of chromosome aberration initially-induced in prematurely condensed chromosomes (PCC) by multicolor-fluorescence *in situ* hybridization (M-FISH). Our results show both simple and complex aberrations to be induced in a LET and dose-dependent manner, and the frequency and complexity of aberration induced to be low in comparison to more spherical cell types, possibly reflecting the ellipsoid geometry of the NHBE nucleus. Based on these data, the long-term transmission of this damage may be possible in ~1–2% of the exposed cell population.

Materials and methods

Cell culture and irradiation

We sourced normal human bronchial epithelial cells (NHBE cells) from Lonza Biologics plc, Slough, UK (Lonza is a Food and Drug Administration (FDA)-approved tissue bank) which had been isolated from human donors (Donor I [Lot number 6F4181] and Donor 2 [Lot 4F1624]) with full donor consent. These cells are representative of the target tissue for exposure to both inhaled α-emitters and normal cells at the periphery of, for example, breast or lung radiation treatment fields. NHBE cells were maintained according to the suppliers recommendations in T75 flasks (Nunc, Fisherbrand, UK) at a density of 3.5×10^3 cells/cm^2 in 15 ml complete Bronchial Epithelial cell Basal Medium (BEBM) [Lonza Bullet kit CC-3170; BEBM is supplemented with retinoic acid (0.1%), human epidermal growth factor (0.1%), epinephrine (0.1%), transferrin (0.1%), triiodothyronine (0.1%), insulin (0.1%), hydrocortisone (0.1%), bovine pituitary extract (0.2%) and gentamicin/amphotericin-B (0.1%) by addition of SingleQuots™ (Lonza)]. Cells were passaged between 80–90% confluence (generally ~4 days in culture (~1–1.5 $\times 10^6$ cells total)), as recommended by the supplier, and refed every 48 h. For this, medium was removed and the cells passaged using

ReagentPack™ Subculture kit (Lonza). In brief, the cell sheet washed in ~10 ml of 25 mM N′-2-hydroxyethylpiperazine-N′-2 ethanesulphonic acid (HEPES) buffer before addition of ~6 ml of trypsin/ethylenediaminetetraacetic acid (EDTA) solution (0.25 μg/ml) for ~4 min, followed by the addition of 12 ml trypsin neutralizing solution (TNS) (Lonza). Cells were centrifuged at 220 *g* for 5 min then re-suspended in complete BEBM. Cells were frozen in 10% dimethyl sulfoxide (DMSO, Sigma-Aldrich, Dorset, UK) for long-term storage from passage 3 (p3).

Cell morphology measurements were made on live NHBE cells incubated in 100 nM of the mitochondrial stain 3,3′-dihexyloxacarbocyanine iodide (DiOC$_6$, Invitrogen Corporation, Carlsbad, CA, USA) 10 min prior to collecting three-dimension (3D) images using a Confocal Laser Scanning microscope. Multiple measurements of the cell and nuclear area were made on 3D images stacks collected for 20 cells using ImageJ software (Rasband, W.S., National Institutes of Health, Bethesda, MD, USA; http://imagej.nih.gov/ij/, 1997–2012). The shape of the nucleus within the cell is approximately an oblate spheroid with an average height of 3.4 μm (standard deviation (SD) = 1.1 μm) and with diameter 11.6 μm (SD = 1.6 μm), corresponding to an average nuclear area of 105 μm^2 (SD = 30 μm^2).

For γ-irradiations, NHBE cells were irradiated as a monolayer at 80–90% confluency using the ^{60}Co source at Brunel University at room temperature (RT) at dose rate of 0.0944 Gy/min. For α-particle irradiations, the NHBE cells were passaged and seeded onto Hostaphan-based (0.35 mg cm^{-2} polyethylene terephthalate; Hoeschst, Weisbaden, Germany) glass-walled dishes (30 mm internal diameter) for 24 h and then transferred, in a portable incubator at 37°C, to the Gray Institute for Radiation Oncology & Biology in Oxford. The cells were then maintained in a humidified gassed (5% CO$_2$/95% air) incubator at 37°C as standard for a further 24–48 h before being irradiated at RT as an attached monolayer at 80–90% confluency with 3.26 megaelectron volt (MeV) α-particles (LET of 121 kiloelectron volt [keV]/μm) using a ^{238}Pu α-particle irradiator described previously (Goodhead et al. 1991). For the M-FISH chromosome aberration study the cells were exposed to a dose of 0.19 Gy (~0.1 Gy/min) which corresponds to a mean of 1.03 high-LET α-particle traversal per cell nucleus for a nuclear area of 105 μm^2 (actual number of nuclear traversals follows a Poisson distribution where 35.7, 36.8, 18.9 and 8.6% of nuclei are traversed by 0, 1, 2 or ≥ 3 tracks).

Fluorescence assisted cell sorting (FACS) analysis

NHBE cells (Donor 2) were trypsinized, centrifuged and washed in 1 ml phosphate buffered saline (PBS, Life Technologies, Carlsbad, CA, USA). Cells were then re-suspended in 500 μl PBS and fixed in ice cold ethanol (70%). The cells were washed in PBS, treated with RNase A (0.1 mg/ml, Sigma-Aldrich) and stained with propidium iodide (40 μg/ml, Sigma-Aldrich) for 30 min at 37°C. Analysis was carried out by flow cytometry using a COULTER EPICS XL-MCL (Beckman Coulter, High Wycombe, Bucks, UK) flow cytometer with EXPO32™ ADC software.

Survival assay

NHBE cells (Donors 1 and 2) were maintained and irradiated as described above with sham, 2, 4, 6 and 8 Gy γ-rays or sham and nominal doses of 0.5 and 1 Gy α-particles. After irradiation, cells were left to recover for ~1 h at 37°C before being passaged and seeded at varying densities. Preliminary experiments highlighted difficulties in supporting NHBE cells in media without replenishment over a two-week period and therefore the scoring of surviving colonies of greater than 50 cells. NHBE cells could however be supported over 8–10 days enabling colonies of greater than 25 cells to be generated. Consequently cells were returned to the incubator after irradiation and left undisturbed for 10 days at 37°C. Surviving cells were fixed in 100% ethanol (Hayman Limited, Essex, UK) and stained with 1% methylene blue (Sigma-Aldrich) in 50% ethanol and scored for the number of surviving colonies. Our criterion for the determination of a surviving colony was any colony of 25 or more cells.

$$\text{Plating efficiency (PE)} = (\text{colonies counted/total cells seeded}) \times 100$$

$$\text{Surviving fraction} = \text{colonies counted/(cells seeded} \times \text{PE)}$$

Premature condensed chromosome (PCC) spreads

NHBE cells (Donor 2) were seeded and irradiated with either low-LET γ-rays or high-LET α-particles as a monolayer at 80–90% confluency, as previously described. After irradiation, NHBE cells were allowed to recover for 1 h at 37°C then passaged and seeded at a density of 3.5×10^3 cells/cm^2 in fresh complete BEBM, containing 10 μM 5′-bromodeoxyuridine (BrdU, Sigma-Aldrich), onto flame sterilized 'superfrost' glass microscope slides (ThermoFisher Scientific, Loughborough, UK) housed within individual quadriperm chambers (Sarstedt, Postfach, Germany). The cells were then cultured for finite periods of time and harvested to achieve the optimal collection of 1st post-irradiation metaphases by adding 40 ng/ml colcemid (Life Technologies) for the final 5 h of the culture time. Calyculin A (50 nM) (Wako Chemicals GmbH, Neuss, Germany) was added 30 min before fixation to induce PCC in G2 cells. The medium was then discarded and the cells incubated in hypotonic solution (0.075 M potassium chloride, Fisher Scientific, Loughborough, Leicestershire UK) at 37°C for 15 min before being fixed by gently washing the microscope slides with ice-cold 3:1 volume to volume: ratio (v:v) methanol:acetic acid (VWR International, Leuven, Belgium) for ~3–5 min. Slides were dried individually on a humidified hot-plate to obtain well spread quality chromosome preparations and stored in an air-tight container at −20°C until required to be stained by either the Harlequin stain or M-FISH painting methods.

Harlequin stain

Slides prepared by the *in situ* harvest method were aged in the dark for a minimum of 3 days then incubated in 20 μg/ml Hoechst 33258 (Sigma-Aldrich) for 10 min before being transferred into 2 × saline-sodium citrate salt solution (SSC, Fisher Scientific), composed of 300 mM sodium chloride and 30 mM tri-sodium citrate and exposed to 20 joules per second ultraviolet light (UV) light for 25 min. The slides were then washed in distilled water and stained with 4% Giemsa (Sigma-Aldrich) in pH 6.8 buffer (Merck, Darmstadt, Germany) for 3–5 min. First, second and third cell division chromosome spreads, since the addition of 5-Bromo-2′-deoxyuridine (BrdU, Sigma-Aldrich), were distinguished according to their chromatid Harlequin stain pattern (Perry and Wolff 1974, Sumption et al. 2006) using brightfield microscopy. The optimal culture time for the collection of 1st cell division metaphase + G2 PCC (termed PCC) spreads (>95% of all spreads) was subsequently ascertained in parallel cultures to be 24 h after irradiation.

Multiplex fluorescence *in situ* hybridization (M-FISH) assay

A modified method of the Metasystems™ protocol was used. To do this, fresh slides of chromosome preparations were hardened (3:1 methanol:acetic acid for 1 h, dehydrated through an ethanol series (2 min each in 70%, 70%, 90%, 90% and 100%), baked at 65°C for 20 min, then 10 min in acetone (VWR International) and pre-treated with 100 μg/ml RNase A (Sigma-Aldrich) in 2 × SSC at 37°C for 1 h prior to washing for 5 min in 2 × SSC.

For hybridization, 10 μl of MetaSystems™ 24-color probe cocktail (MetaSystems, Altlussheim, Germany) was denatured by incubating at 75°C for 5 min. After this time, the probe was placed onto ice briefly then incubated at 37°C for 30 min. In parallel, slides were incubated in 0.1 × SSC for 1 min at RT, 2 × SSC for 30 min at 70°C and 0.1 × SSC for 1 min at RT. The slides were then denatured in 0.07N sodium hydroxide for 1 min at RT, before being washed sequentially in 0.1 × SSC at 4°C and 2 × SSC at 4°C for 1 min each and dehydrated through an ethanol series of 30, 50, 70, and 100% for 1 min each. Cells and probe were then mixed and left to hybridize for 48–72 h at 37°C before being washed in 1 × SSC at 73°C for 5 min and 4 × SSC/0.05% Tween20 (Fisher Scientific) at RT for 5 min. A mix of 50 μl blocking reagent (MetaSytems) containing 1 μl Metasystems™ detection agent was then applied to the slide and overlaid using a 22 × 40 mm^2 coverslip (Menzel-Glaser, Braunschweig, Germany) and incubated at 37°C for 15 min. After this time, the slide was washed sequentially in 4 × SSC containing 0.05% Tween20 and PBS at RT for 3 min each, then left to dry in the dark at RT. Cells were counterstained using 4′,6-diamidino-2-phenylindole (DAPI III) (MetaSystems), sealed and stored in the dark at −20°C.

M-FISH analysis

Chromosome aberrations were analyzed as previously described (Anderson et al. 2003). In brief, PCC spreads were visualized using an 8-position Zeiss Axioplan II fluorescence microscope (Carl Zeiss, Oberkochen, Germany) containing individual filter sets for each component fluor of the Metasystems™ probe cocktail plus DAPI. Digital images are captured for M-FISH using a charged-coupled device (CCD) camera (Photometrics Sensys CCD, Tucson, AZ, USA) coupled to and driven by Metasystems™ ISIS fluorescence imaging system software. In the first instance, cells were karyotyped and analyzed by enhanced DAPI banding.

Detailed paint analysis was then performed by assessing paint coverage for each individual fluor down the length of each individual chromosome, using both the raw and processed images for each fluor channel. A PCC spread was classified as being apparently normal if all 46 chromosomes were observed by this process, and subsequently confirmed by the Metasystems™ M-FISH assignment, to have their appropriate combinatorial paint composition down their entire length.

Classification of chromosome aberrations

Structural chromosomal abnormalities were identified as color-junctions down the length of individual chromosomes and/or by the presence of chromosome fragments. The M-FISH paint composition was used to identify the chromosomes involved in the abnormality and assignment of a breakpoint to a specific chromosomal region (pter, p, peri-centromere, q or qter) was based on the DAPI banding pattern at the M-FISH colour junction, the location of the centromere and the size of the painted material on each rearranged chromosome. A detailed assignment of breakpoints to chromosome bands was not possible due to limits in DAPI resolution and no attempt was made to consider intrachromosomal events such as inversions.

Exchange aberrations involving three or more breaks in two or more chromosomes were classed as *complex* and assigned the minimum C/A/B (number of different chromosomes/arms/breaks) required to produce the visible complex (Savage and Simpson 1994). The potential transmissibility of each complex (based on the presence or absence of unstable elements such as dicentrics and acentric fragments in the complex rearrangement) was also detailed. Exchange aberrations involving only two breaks in one or two chromosomes were classified as *simple* and further characterized as stable reciprocal translocations, unstable dicentrics or centric rings. For all simple and complex exchanges, the completeness of the exchange was recorded as complete (all break-ends rejoined), true-incomplete (where one or more break-ends fail to find an exchange partner) or one-way (where one or more elements appear to be missing) (Boei and Natarajan 1998, Cornforth 2001). PCC breaks not involved in an exchange were classified as terminal deletions if they were accompanied by a linear acentric fragment (this fragment was further categorized as being either proximate or non-proximate to the broken chromosome), as truncated if no associated fragment was visible and, as excess acentric fragments.

Abnormalities were classified as clonal if the same chromosome aberration, involving breakpoints in the same regions, were observed in two (or more) spreads. A PCC spread was categorized as stable only if all of the abnormalities detected within that spread were classified as stable.

Results

Normal human bronchial epithelial (NHBE) cells are primary human cells capable of only a finite number of population doublings (P.D). Supplementary Figure 1A (to be found online at http://informahealthcare.com/abs/doi/10.3109/09

553002.2013.805889) shows the exponential growth of NHBE cells over 30 days representative of 19 P.D and ~8 passages (p2–p8). Morphologically NHBE cells retain their characteristic epithelia shape (Supplementary Figure 1B, to be found online at http://informahealthcare.com/abs/doi/10.3109/09553002.2013.805889) if routinely passaged around ≤90% confluency; however, the growth rate will reduce and larger, more spherical (goblet) cell types (Supplementary Figure 1C to be found online at http://informahealthcare.com/abs/doi/10.3109/09553002.2013.805889) will predominate if cultures are left to reach 100% confluency before passage. Accordingly, NHBE cells could not be irradiated in a plateau contact-inhibited (G_o) phase. Furthermore, the strict culture regime required by these cells limited the opportunity for cell synchronization by, for example, growth factor starvation. We therefore sampled NHBE cells in exponential growth and determined their population cell cycle status by FACS analysis finding that ~80% of NHBE cells were in G_o/G_1 when cultured to ~90% confluency. Accordingly, all irradiations were carried out at ~90% confluency.

Figure 1 plots the survival of NHBE cells irradiated with high-LET α-particles or ^{60}Co γ-irradiation. The plating efficiency of NHBE cells was found to be ~ 26% and consistent with that obtained by the cell suppliers (Lonza).

Characterization of chromosome aberrations in NHBE cells

We elected to irradiate early passage NHBE (p3/p4) cells in an effort to more closely mimic the damage response in 'primary' cells rather than in populations that have been repeatedly passaged *in vitro*. However, the total number of cells available for experimentation at early passage is limited and insufficient for suspension harvest methodology. In addition, preliminary experiments showed NHBE cells to be refractory to standard colcemid treatment for the collection of mitotic chromosomes with mitotic indices achieved of <1%. Accordingly, irradiated cells were seeded onto glass microscope slides for culture and treatment for the premature condensation of chromosomes (PCC) *in situ*.
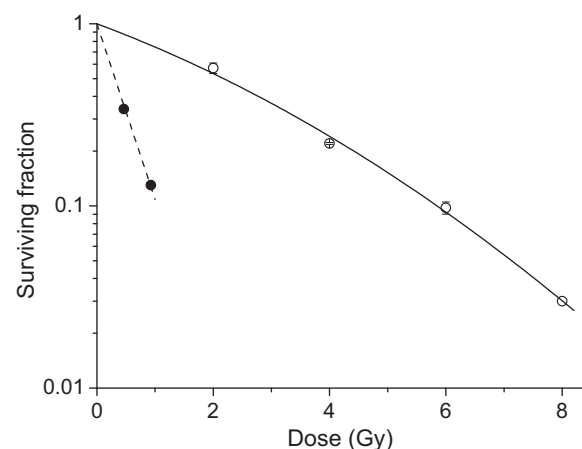

Figure 1. Survival curve for NHBE cells following exposure to high-LET α-particles (circle) and ^{60}Co γ-rays (square; error bars represent standard deviation, $n = 3$). The variation in surviving fraction, S, as a function of dose, D, was fitted to equation $S = \exp(-\alpha D - \beta D^2)$ where $\alpha = 2.22 \pm 0.02$ and $\beta = 0$ for alpha-particles and $\alpha = 0.27 \pm 0.03$ and $\beta = 0.021 \pm 0.004$ for γ-rays.

Table I. Frequency of chromosomal damage induced in NHBE cells after exposure to γ-rays.

| Test | Total cells | Frequency Abnormal | Frequency Simple | | | | Frequency Complex | | | | Frequency PCC breaks |
			Total	Complete	True-incomplete	One-way	Total	Complete	True-incomplete	One-way	Total
Sham	171	0.123	0.006	0	0.006	0	0	0	0	0	0.170
0.5 Gy	179	0.168	0.061	0.022	0	0.039	0.011	0	0	0.011	0.151
1.0 Gy	106	0.217	0.106	0.047	0	0.057	0.038	0	0	0.038	0.198

Induction of chromosome aberrations after exposure to γ-rays

Table I details the frequency and type of chromosome aberration observed by M-FISH to be initially-induced in NHBE cells after exposure to sham, 0.5 and 1 Gy low-LET ^{60}Co-γ-rays and shows that both simple and complex exchange types were induced after radiation exposure. Specifically, the frequency of simple exchanges induced was significantly greater after exposure to 0.5 and 1 Gy compared to sham ($p < 0.004$) while a significantly greater frequency of complexes were induced again compared to sham (0.00) after exposure to 1 Gy (0.038, $p = 0.04$) but not 0.5 Gy (0.011, $p = 0.17$). The total background frequency of damage (0.176) observed in NHBE cells predominantly represents PCC-breaks (0.170) of which ~ 40% comprise terminal deletions lying in close alignment with their associated painted fragment (Table II). A similar frequency ($p > 0.5$) and trend in fragment alignment was also observed after exposure to γ-rays (Table II), which is in keeping with observations by George et al. (2009), accordingly a proportion of PCC breaks are suggested to be artefacts of the calyculin A treatment. Given this and the lack of any true-incomplete exchanges (Table I), it is likely that the majority of all γ-ray-induced breaks were repaired (either correctly or incorrectly) by the time of sampling (Cornforth and Bedford 1983).

Induction of chromosome aberrations after exposure to high-LET α-particles

Table III details the frequency and type of chromosome aberration initially-induced in NHBE cells 24–34 h after exposure to ~ 1 α-particle/nucleus high-LET α-particles (3.26 MeV, 121 keV/μm) and shows that both simple and complex exchange types were induced.

Significantly elevated frequencies of simple (0.156, $p = 0.0004$) and complex (0.096, $p = 0.004$) aberrations were observed 24 h after exposure to ~ 1 α-particle/nucleus,

giving a simple:complex (S:C) ratio of ~ 1.6 (equivalent to ~ 40% of exchanges classified as complex). We also observed an elevated frequency of PCC-breaks (0.709) compared to sham (0.184, $p = 0.0002$) suggesting incomplete repair of α-particle-induced damage at the time of PCC condensation. To assess this, we extended our study to characterize the complexity of aberration observed in delayed (29 and 34 h after exposure) 1st cell division PCC spreads determined using Harlequin staining (parallel cultures revealed ~ 95% of cells to be in 1st cell division by 34 h). We found that the PCC break frequency did decline with culture time (chromosome break frequencies of 0.709, 0.310 and 0.370 for 24, 29 and 34 h, respectively) after irradiation but did not reach the same frequency as sham levels (pooled background frequency 0.145), suggesting some α-particle-induced damage in NHBE cells remains unrepaired up to 34 h after exposure. To support this argument and in contrast to that after γ-rays (Table I), we categorized 36 and 37% of all simple and complex exchanges, respectively, as 'true-incomplete' types up to 29 h after exposure (Table III). Thus, α-particle-induced damage remains available to be correctly or incorrectly repaired and therefore possibly resolved as chromosome exchanges, in delayed 1st division cells. To assess whether such a delay was associated with an increase in aberration complexity, we examined the number and complexity of each aberration in each damaged cell. No difference in the frequency of simple ($p > 0.16$) or complex ($p > 0.19$) exchanges between fixation times was detected, with the exception of a lower complex frequency 29 h after exposure compared to 24 h ($p = 0.01$). Additionally, we found no evidence for any increase in aberration complexity with increasing length of culture time based on the fraction of complex aberrations observed (S:C ratios of 1.6, 2.8, 1.6 for 24, 29 and 34 h, respectively) (Table III), the minimum size of each complex exchange (Table IV) or damaged cell burden (Figure 3).

Table II. Frequency and sub-classification of PCC breaks.

| Test | Cells | Frequency of PCC break types | | | | |
| | | Total | Terminal deletion | | Truncated chromosome | Excess fragments |
			Proximal	Non-proximal		
Sham	171	0.170	0.070	0.064	0.035	0
0.5 Gy γ-rays	179	0.151	0.056	0.045	0.045	0.006
1 Gy γ-rays	106	0.198	0.047	0.094	0.038	0.019
Sham pooled	422	0.145	0.047	0.050	0.038	0.009
~ 1 α-particle/nucleus						
24 h	230	0.709	0.209	0.339	0.057	0.104
29 h	313	0.310	0.102	0.141	0.042	0.026
34 h	139	0.367	0.058	0.165	0.115	0.029
Pooled	682	0.456	0.129	0.213	0.062	0.053

Table III. Frequency of chromosomal damage induced in NHBE cells after exposure to ~1 α-particle/nucleus.

Test	Total cells	Frequency Abnormal	Frequency Simple				Frequency Complex				Frequency PCC breaks Total
			Total	Complete	True-incomplete	One-way	Total	Complete	True-incomplete	One-way	
Sham											
24 h	103	0.126	0	0	0	0	0	0	0	0	0.184
29 h	196	0.147	0.015	0	0	0.015	0	0	0	0	0.194
34 h	123	0.041	0.016	0	0	0.016	0	0	0	0	0.033
Pooled	422	0.111	0.012	0	0	0.012	0	0	0	0	0.145
~1 α-particle/nucleus											
24 h	230	0.443	0.156	0.061	0.047	0.047	0.096	0.008	0.043	0.043	0.709
29 h	313	0.275	0.105	0.032	0.038	0.035	0.035	0.009	0.013	0.013	0.310
34 h	139	0.345	0.108	0.036	0	0.072	0.065	0	0.029	0.036	0.370
Pooled	682	0.346	0.123	0.043	0.034	0.047	0.062	0.007	0.026	0.028	0.456

Distribution of chromosome damage

To assess how the chromosomal exchanges in Tables I and III are distributed throughout each damaged cell we have categorized the frequency of spreads that contain one, two or > two independent simple or complex exchanges (Figures 2 and 3).

Figure 2 shows that all of the cells observed to be damaged after exposure to 0.5 Gy γ-rays contain just one simple or complex exchange while ~ 30% of damaged cells contain multiple exchanges (e.g., simple + simple or simple + complex) after exposure to the higher dose of 1.0 Gy γ-rays. Therefore, although the overall frequency of exchanges is lower after exposure to 0.5 Gy (Table I), it is likely that a greater relative fraction of induced aberrations will be capable of long-term persistence. This is based on the likelihood that aberrations classed as stable may be present in cells that also contain unstable aberrations at the higher dose of 1 Gy. This trend of multiple independent exchanges being induced in individual cells is even more striking after α-particle exposure, with similar implications for reduced frequencies of induced aberrations being capable of long-term persistence (Figure 3).

Transmissibility of radiation-induced chromosome aberrations

The transmission potential of induced aberrations was determined by classifying all exchanges observed in Tables I

Table IV. Minimum number of chromosomes and breaks in each complex exchange.

Minimum number/complex		Low-LET γ-rays Frequency observed		~ 1 high-LET α-particle/nucleus Frequency observed		
Chromosomes	Breaks	0.5 Gy	1.0 Gy	24 h	29 h	34 h
2	3	–	0.250	0.017	0.013	0.007
	4	0.500	–	0.017	0.003	–
	5	–	–	0.004	–	0.007
3	3	–	0.250	0.017	0.010	0.007
	4	–	0.250	0.017	–	0.022
	5	–	–	0.009	–	–
4	3	–	–	–	–	–
	4	0.500	–	–	0.006	0.014
	5	–	–	0.004	–	–
5	6	–	–	–	–	0.007
	7	–	–	–	–	–
	8	–	–	0.004	–	–
6	6	–	0.250	–	–	–
	7	–	–	0.004	–	–

and III into stable or unstable types (as described in *Methods*). Table V shows the frequency of complete reciprocal translocations to be 0.017, 0.047 and 0.032 (or 0.045, 0.094 and 0.063 if one-way translocations are also considered) after exposure to 0.5 Gy γ-rays, 1.0 Gy γ-rays and 1 high-LET α-particle/nucleus respectively. No transmissible complex aberrations were observed in either population exposed to γ-rays, however a frequency of 0.001 (or 0.010 if one-way exchanges are also considered) was observed after α-particle exposure (Table V). In addition to this, the transmission potential of each damaged cell was determined based on the stability of all complete exchanges observed in each cell (data not shown), revealing very similar transmissible frequencies of 0.017, 0.019 and 0.016 after exposure to 0.5 Gy γ-rays, 1.0 Gy γ-rays and 1 high-LET α-particle/nucleus, respectively.

Discussion

The purpose of this work was to gain a better understanding of the frequency and types of chromosome aberration initially-induced in human lung cell types to: (1) Link initial damage and rearrangements with transmission potential and assess how this varies for low-LET γ-rays and high-LET α-particle exposures, and (2) to further understanding of the mechanisms of chromosome aberration formation. To do this, we exposed normal human bronchial epithelial (NHBE, Lonza) cells *in vitro* to low-LET γ-rays and a low fluence of high-LET α-particles and then carried out detailed cytogenetic examination of the damage induced by assaying PCC spreads by M-FISH. NHBE cells are isolated from the bronchial epithelial surface of donors undergoing surgery for unrelated conditions, are untransformed and have a stable diploid karyotype. Importantly this cell type is representative of the target tissue from environmental, occupational and medical sources of radiation exposure.

Both simple and complex aberrations were observed 24 h after exposure to high-LET α-particles (~1 α-particle/nucleus) (S:C ratio ~1.6) and low-LET γ-rays (1 Gy) (S:C ratio ~2.8); however, only simple exchanges were detected at appreciable levels above sham at the lower dose of 0.5 Gy γ-rays (Tables I and III). These data are consistent with expectations that the deposition of damage by doses of less than ~1 Gy of sparsely ionizing radiation may only rarely result in
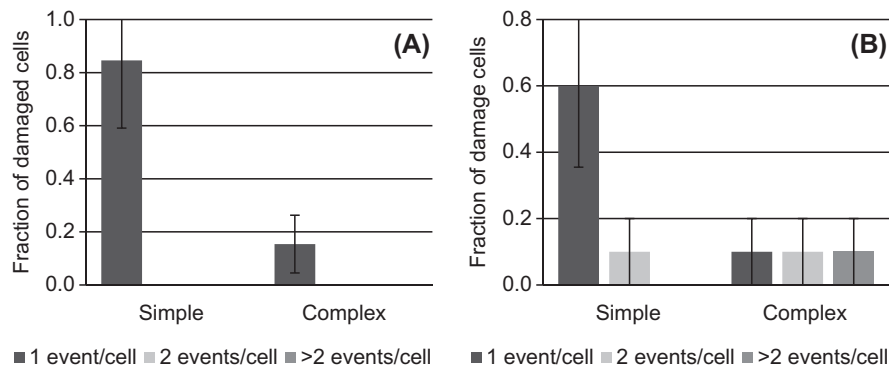
Figure 2. Distribution of chromosomal exchanges in aberrant spreads observed 24 hours after exposure to (A) 0.5 or (B) 1.0 Gy γ-rays. The fraction of damaged cells that contain 1 (dark), 2 (light) or > 2 (medium) simple exchanges (simple) or simple + complex exchanges (complex) are shown. Error bars represent standard deviation.

a complex rearrangement (e.g., involving multiple breaks in two or more different chromosomes) (Loucas and Cornforth 2001) in contrast to low doses (equivalent to a fluence of 1 track/nucleus) of densely ionizing α-particles (Griffin et al. 1995, Anderson et al. 2000). Accordingly and in keeping with other studies, the complexity of radiation-induced chromosome aberrations induced in NHBE cells is dependent on radiation quality and dose (Boei et al. 2001, George et al. 2001, Ritter et al. 2010).

The proportion of all exchanges classified as complex 24 h after exposure to high-LET α-particles was ~ 40% (S:C ratio 1.6), in-line with that observed in fibroblast cells (Griffin et al. 1995, Durante et al. 2010, Loucas et al. 2013) but which is in contrast to previous M-FISH studies examining an equi-fluence (1 track/nucleus) of α-particle-induced aberration

complexity in peripheral blood lymphocytes (PBL) (Anderson et al. 2002, 2006) and haemopoeitic stem cells (HSC) (Anderson et al. 2007), where the S:C ratio was < 1. The reduced complexity in NHBE cells may be a reflection of the relationship between the delayed formation of exchanges in heavily damaged cells (George et al. 2001, Ritter et al. 2002b, 2002a, Anderson et al. 2003) whereby exchanges of increasing complexity are observed at later sampling times (Lee et al. 2010). Indeed we did observe an ongoing decline in the PCC break frequency with culture time (Table II) and ~ half of all the incomplete simple exchanges were classified as 'true-incomplete' up to 29 h after exposure (Table III), suggesting that a fraction of α-particle-induced damage in NHBE cells remains unrepaired up to 34 h after exposure (Goodwin et al. 1994, Durante et al. 1998, Suzuki et al. 2001, Wu et al.
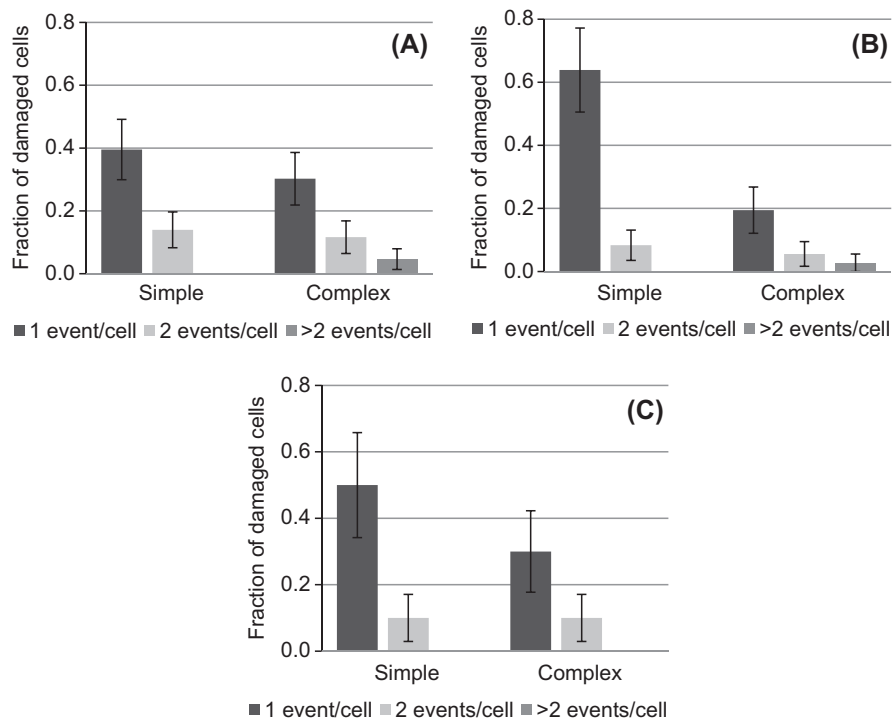

Figure 3. Distribution of chromosomal exchanges in aberrant spreads observed (A) 24, (B) 29 and (C) 34 hours after exposure to ~ 1 high-LET α-particle/nucleus. The fraction of damaged cells that contain 1 (dark), 2 (light) or > 2 (medium) simple exchanges (simple) or simple + complex exchanges (complex) are shown. Error bars represent standard deviation.

Table V. Simple and complex exchanges classified as transmissible.

Test	Cells	Reciprocal translocation (2B)			Transmissible complex		
		Total	Complete	One-way	Total	Complete	One-way
Sham pooled	490	0.010	0	0.008	0	0	0
0.5 Gy γ-rays	179	0.045	0.017	0.028	0	0	0
1 Gy γ-rays	106	0.094	0.047	0.047	0	0	0
~1 α-particle/nucleus							
Pooled	682	0.087	0.032	0.031	0.013	0.001	0.009

2003b). This would be consistent with the densely ionizing structure of an α-particle track not only resulting in complex DNA double-strand breaks (a DSB with associated additional damage sites within a few base pairs) but also, a correlation of DSB sites across nucleosomes or chromatin fibre resulting in small DNA fragments and potentially impacting on the efficiency of repair (Lobrich et al. 1996, Alloni et al. 2012). In terms of complexity however, no increase in the fraction of exchanges classified as complex (Table III), complexity of each complex exchange (Table IV) or aberration burden of each delayed cell (Figure 3) was observed, when NHBE cells exposed to α-particles were cultured for increasing lengths of time. The excess of PCC breaks that remain by 34 h may of course reflect excessively delayed 1st division cells containing damage of increased complexity; however, it is unlikely this could account for such a reduction in complexity of aberration observed. Therefore complex chromosome aberrations are not the dominant exchange-type in NHBE cells exposed *in vitro* to high-LET α-particle radiation in a set-up where the α-particles hit perpendicularly. The small proportion of non-G_1 cells present at time of irradiation and/or differences in repair fidelity may be relevant in explaining this finding but also pertinent is that NHBE cells are ellipsoid in shape and geometrically flatter than PBL or HSC, meaning that the relative 3-D organization of individual chromosome territories will be different to that for spherical PBL and HSC. NHBE cells therefore irradiated with α-particles through the base of the dish (as in this study), would be expected to have fewer chromosome territories intersected (and also fewer total DSB) than if they were irradiated across their length for example. Accordingly, these data support the proposal that the complexity of aberration initially-induced by particulate radiation may also be related to the number of chromosome territories intersected (Anderson et al. 2006, Foster et al. 2013). Indeed a recent study demonstrates this directly by showing varying fractions of complex aberration to be induced in human AG1522 fibroblasts depending on the path of exposure through the ellipsoid nucleus (Durante et al. 2010).

In addition to this, the frequency of simple exchanges induced in NHBE cells after exposure to γ-rays (Table I) is lower to that previously observed in PBL. For instance, simple exchanges were observed by M-FISH to be to be induced at a frequency of ˜ 0.240 (Loucas and Cornforth 2001, Loucas et al. 2013) and 0.320 (Ritter et al. 2010) after exposure of PBL to 1 Gy γ-rays while Golfier et al. (2009) observed a dicentric (only) frequency of 0.086 and 0.18 after exposure to 0.6 and 1 Gy, respectively (Golfier et al. 2009). Although in contrast to Loucas et al. (2013), our results for the induction of

simples are consistent with that observed in HF19 fibroblasts whereby frequencies of 0.022, 0.031 and 0.054 were detected after exposure to 0.25, 0.5 and 1 Gy, respectively (George et al. 2009). Thus, there is an apparently higher frequency of simple exchanges induced in spherical PBL compared to ellipsoid NHBE cells suggesting it is possible that cellular geometry, where relatively more surface area of each chromosome territory neighbors another chromosome territory in spherical nuclei, compared to more flattened types (where a greater proportion of the territories are likely to be at the periphery of the nucleus), is also relevant for the induction of aberrations of varying complexities after γ-rays (in this case interchanges rather than intrachanges) as discussed for α-particle exposure (Foster et al. 2013).

The stability of a damaged cell is influenced by many factors including the stability of any aberrations initially-induced. Therefore in an effort to assess the long-term transmission potential of damaged NHBE cells we classified all chromosome exchanges initially-induced by γ-rays (Table I) and α-particles (Table III) according to whether they were stable and capable of transmission through cell division (Table V). The frequencies of γ-ray-induced stable translocations were found to be slightly lower (0.017 and 0.047 for 0.5 and 1 Gy, respectively) than published studies, most likely reflecting the reduced frequency of aberrations initially-induced (Table I). For instance, simple frequencies of 0.31 and 0.15 were observed by M-FISH to persist through long-term cultures after exposure to 2 and 4 Gy γ-rays (Duran et al. 2009) while we previously observed a frequency of 0.2 by three-color FISH in PBL ~20 days after exposure to 3 Gy γ-rays (Anderson et al. 2003). Similarly, the transmission potential of damaged cells was low after exposure to γ-rays (0.017 and 0.019) although comparable to that observed after α-particle (0.016) exposure. Multiple exchanges induced in the same cell (Figures 2 and 3) whereby additional unstable damage contributes to the decline in stable exchanges over time may influence this (Matsumoto et al. 1998, Tawn and Whitehouse 2003). Thus, only ~1–2% of all exposed cells are likely to be capable of transmitting radiation-induced chromosomal damage to future NHBE cell generations, irrespective of dose.

In conclusion, the frequency and complexity of chromosome aberrations induced in NHBE cells varies with radiation quality and dose, and overall, is lower to that previously observed in spherical cell types after exposure to comparable doses or fluence of radiation. One possible mechanistic explanation for this is the geometric organization of chromosome territories within ellipsoid nuclei. If valid, these findings add to the story of the importance of understanding

nuclear geometry and how this may impact on the potential transmission of induced aberrations and, determination of tissue-specific radiation risk estimates. Indeed the influence of the 3D tissue architecture on the complexity of aberration induced and how this may be different in comparison to monolayer cell cultures needs to be examined in order to more accurately correlate to *in vivo* exposures.

Declaration of interest

The authors report no conflicts of interest. The authors alone are responsible for the content and writing of the paper.

References

Alloni D, Campa A, Friedland W, Mariotti L, Ottolenghi A. 2012. Track structure, radiation quality and initial radiobiological events: Considerations based on the PARTRAC code experience. International Journal of Radiation Biology 88:77–86.

Anderson RM, Stevens DL, Goodhead DT. 2002. M-FISH analysis shows that complex chromosome aberrations induced by alpha-particle tracks are cumulative products of localized rearrangements. Proceedings of the National Academy of Science of the USA 99:12167–12172.

Anderson RM, Papworth DG, Stevens DL, Sumption ND, Goodhead DT. 2006. Increased complexity of radiation-induced chromosome aberrations consistent with a mechanism of sequential formation. Cytogenetics and Genome Research 112:35–44.

Anderson RM, Marsden SJ, Wright EG, Kadhim MA, Goodhead DT, Griffin CS. 2000. Complex chromosome aberrations in peripheral blood lymphocytes as a potential biomarker of exposure to high-LET alpha-particles. International Journal of Radiation Biology 76:31–42.

Anderson RM, Stevens DL, Sumption ND, Townsend KM, Goodhead DT, Hill MA. 2007. Effect of linear energy transfer (LET) on the complexity of alpha-particle-induced chromosome aberrations in human CD34 + cells. Radiation Research 167:541–550.

Anderson RM, Marsden SJ, Paice SJ, Bristow AE, Kadhim MA, Griffin CS, Goodhead DT. 2003. Transmissible and nontransmissible complex chromosome aberrations characterized by three-color and mFISH define a biomarker of exposure to high-LET alpha particles. Radiation Research 159:40–48.

Beels L, Bacher K, De Wolf D, Werbrouck J, Thierens H. 2009. Gamma-H2AX foci as a biomarker for patient X-ray exposure in pediatric cardiac catheterization are we underestimating radiation risks? Circulation 120:1903–1909.

Boei JJ, Natarajan AT. 1998. Combined use of chromosome painting and telomere detection to analyse radiation-induced chromosomal aberrations in mouse splenocytes. International Journal of Radiation Biology 73:125–133.

Boei JJ, Vermeulen S, Mullenders LH, Natarajan AT. 2001. Impact of radiation quality on the spectrum of induced chromosome exchange aberrations. International Journal of Radiation Biology 77:847–857.

Bonassi S, Norppa H, Ceppi M, Stromberg U, Vermeulen R, Znaor A, Cebulska-Wasilewska A, Fabianova E, Fucic A, Gundy S, et al. 2008. Chromosomal aberration frequency in lymphocytes predicts the risk of cancer: Results from a pooled cohort study of 22 358 subjects in 11 countries. Carcinogenesis 29:1178–1183.

Cornforth MN. 2001. Analyzing radiation-induced complex chromosome rearrangements by combinatorial painting. Radiation Research 155:643–659.

Cornforth MN, Bedford JS. 1983. X-ray-induced breakage and rejoining of human interphase chromosomes. Science 222:1141–1143.

Darby S, Hill D, Auvinen A, Barros-Dios JM, Baysson H, Bochicchio F, Deo H, Falk R, Forastiere F, Hakama M, et al. 2005. Radon in homes and risk of lung cancer: Collaborative analysis of individual data from 13 European case-control studies. British Medical Journal 330:223.

Darby S, Hill D, Deo H, Auvinen A, Barros-Dios JM, Baysson H, Bochicchio F, Falk R, Farchi S, Figueiras A, et al. 2006. Residential radon and lung cancer – detailed results of a collaborative analysis of individual data on 7148 persons with lung cancer and 14,208 persons without lung cancer from 13 epidemiologic studies in Europe. Scandinavian Journal of Work Environmental Health 32:1–83.

Duran A, Barquinero JF, Caballin MR, Ribas M, Barrios L. 2009. Persistence of radiation-induced chromosome aberrations in a long-term cell culture. Radiation Research 171:425–437.

Durante M, Pignalosa D, Jansen JA, Walboomers XF, Ritter S. 2010. Influence of nuclear geometry on the formation of genetic rearrangements in human cells. Radiation Research 174:20–26.

Durante M, Furusawa Y, George K, Gialanella G, Greco O, Grossi G, Matsufuji N, Pugliese M, Yang TC. 1998. Rejoining and misrejoining of radiation-induced chromatin breaks. IV. Charged particles. Radiation Research 149:446–454.

Foster HA, Estrada-Girona G, Themis M, Garimberti E, Hill MA, Bridger JM, Anderson RM. 2013. Relative proximity of chromosome territories influences chromosome exchange partners in radiation-induced chromosome rearrangements in primary human bronchial epithelial cells. Mutation Research. Genetic Toxicology and Environmental Mutagenesis. 756:66–77.

George K, Chappell LJ, Cucinotta FA. 2010. Persistence of space radiation-induced cytogenetic damage in the blood lymphocytes of astronauts. Mutation Research-Genetic Toxicology and Environmental Mutagenesis 701:75–79.

George K, Wu H, Willingham V, Furusawa Y, Kawata T, Cucinotta FA. 2001. High- and low-LET induced chromosome damage in human lymphocytes: A time-course of aberrations in metaphase and interphase. International Journal of Radiation Biology 77:175–183.

George KA, Hada M, Jackson LJ, Elliott T, Kawata T, Pluth JM, Cucinotta FA. 2009. Dose response of gamma-rays and iron nuclei for induction of chromosomal aberrations in normal and repair-deficient cell lines. Radiation Research 171:752–763.

Golfier S, Jost G, Pietsch H, Lengsfeld P, Eckardt-Schupp F, Schmid E, Voth M. 2009. Dicentric chromosomes and gamma-H2AX foci formation in lymphocytes of human blood samples exposed to a CT scanner: A direct comparison of dose response relationships. Radiation Protection Dosimetry 134:55–61.

Goodhead DT, Bance DA, Stretch A, Wilkinson RE. 1991. A versatile Pu-238 irradiator for radiobiological studies with alpha-particles. International Journal of Radiation Biology 59:195–210.

Goodwin EH, Blakely EA, Tobias CA. 1994. Chromosomal damage and repair in G1-phase Chinese hamster ovary cells exposed to charged-particle beams. Radiation Research 138:343–351.

Griffin CS, Marsden SJ, Stevens DL, Simpson P, Savage JR. 1995. Frequencies of complex chromosome exchange aberrations induced by 238Pu alpha-particles and detected by fluorescence in situ hybridization using single chromosome-specific probes. International Journal of Radiation Biology 67:431–439.

Hall EJ, Brenner DJ. 2008. Cancer risks from diagnostic radiology. British Journal of Radiology 81:362–378.

International Commission on Radiological Protection (ICRP). 2005. Publication 99: Low-dose extrapolation of radiation-related cancer risk. 99.

Krewski D, Lubin JH, Zielinski JM, Alavanja M, Catalan VS, Field RW, Klotz JB, Letourneau EG, Lynch CF, Lyon JL, et al. 2006. A combined analysis of North American case-control studies of residential radon and lung cancer. Journal of Toxicology and Environmental Health 69:533–597.

Lee R, Sommer S, Hartel C, Nasonova E, Durante M, Ritter S. 2010. Complex exchanges are responsible for the increased effectiveness of C-ions compared to X-rays at the first post-irradiation mitosis. Mutation Research 701:52–59.

Lobrich M, Cooper PK, Rydberg B. 1996. Non-random distribution of DNA double-strand breaks induced by particle irradiation. International Journal of Radiation Biology 70:493–503.

Loucas BD, Cornforth MN. 2001. Complex chromosome exchanges induced by gamma rays in human lymphocytes: An mFISH study. Radiation Research 155:660–671.

Loucas BD, Durante M, Bailey SM, Cornforth MN. 2013. Chromosome damage in human cells by gamma rays, alpha particles and heavy ions: Track interactions in basic dose-response relationships. Radiation Research 179:9–20.

Matsumoto K, Ramsey MJ, Nelson DO, Tucker JD. 1998. Persistence of radiation-induced translocations in human peripheral blood determined by chromosome painting. Radiation Research 149:602–613.

Mitelman F. 2005. Cancer cytogenetics update. http://atlasgeneticsoncology.org/

National Research Council (NRC). 1998. Committee on health risks of exposure to radon (BEIR VI). Health effects of exposure to radon. Washington, DC: National Academy Press.

National Research Council (NRC). 2006. Committee to assess health risks from exposure to low levels of ionizing radiation (BEIR VII). Washington, DC: National Academy Press.

Perry P, Wolff S. 1974. New Giemsa method for differential staining of sister chromatids. Nature 251:156–158.

Peto R, Darby S, Deo H, Silcocks P, Whitley E, Doll R. 2000. Smoking, smoking cessation, and lung cancer in the UK since 1950: Combination of national statistics with two case-control studies. British Medical Journal 321:323–329.

Ritter S, Nasonova E, Gudowska-Novak E. 2002a. Effect of LET on the yield and quality of chromosomal damage in metaphase cells: A time-course study. International Journal of Radiation Biology 78:191–202.

Ritter S, Nasonova E, Furusawa Y, Ando K. 2002b. Relationship between aberration yield and mitotic delay in human lymphocytes exposed to 200 MeV/u Fe-ions or X-rays. Journal of Radiation Research (Tokyo) 43(Suppl.):S175–179.

Ritter S, Lee R, Sommer S, Hartel C, Nasonova E, Durante M. 2010. Complex exchanges are responsible for the increased effectiveness of C-ions compared to X-rays at the first post-irradiation mitosis. Mutation Research-Genetic Toxicology and Environmental Mutagenesis 701:52–59.

Savage JR, Simpson PJ. 1994. FISH 'painting' patterns resulting from complex exchanges. Mutation Research 312:51–60.

Steinfort DP, Einsiedel P, Irving LB. 2010. Radiation dose to patients and clinicians during fluoroscopically-guided biopsy of peripheral pulmonary lesions. Respiratory Care 55:1469–1474.

Sumption ND, Goodhead DT, Anderson RM. 2006. No increase in radiation-induced chromosome aberration complexity detected by m-FISH after culture in the presence of 5′-bromodeoxyuridine. Mutation Research 594:30–38.

Sun S, Schiller JH, Gazdar AF. 2007. Lung cancer in never smokers – a different disease. Nature Reviews Cancer 7:778–790.

Suzuki M, Piao C, Hall EJ, Hei TK. 2001. Cell killing and chromatid damage in primary human bronchial epithelial cells irradiated with accelerated 56Fe ions. Radiation Research 155:432–439.

Tawn EJ, Whitehouse CA. 2003. Persistence of translocation frequencies in blood lymphocytes following radiotherapy: Implications for retrospective radiation biodosimetry. Journal of Radiological Protection 23:423–430.

Taylor ML, Kron. 2011. Consideration of the radiation dose delivered away from the treatment field to patients in radiotherapy. Journal of Medical Physics 36:59–71.

Tomasek L, Placek V. 1999. Radon exposure and lung cancer risk: Czech cohort study. Radiation Research 152:S59–63.

Travis WD, Travis LB, Devesa SS. 1995. Lung-cancer. Cancer 75:191–202.

Wu H, Durante M, Furusawa Y, George K, Kawata T, Cucinotta FA. 2003a. M-FISH analysis of chromosome aberrations in human fibroblasts exposed to energetic iron ions in vitro. Advances in Space Research 31:1537–1542.

Wu H, Durante M, Furusawa Y, George K, Kawata T, Cucinotta FA. 2003b. Truly incomplete and complex exchanges in prematurely condensed chromosomes of human fibroblasts exposed in vitro to energetic heavy ions. Radiation Research 160:418–424.

Xu XG, Bednarz B, Paganetti H. 2008. A review of dosimetry studies on external-beam radiation treatment with respect to second cancer induction. Physics in Medicine and Biology 53:R193–241.

Supplementary material available online

Supplementary Figure 1.